Liquid Crystals
Publication details, including instructions for authors and subscription information:
http://www.informaworld.com/smpp/title~content=t713926090

Investigations on liquid crystalline partially fluorinated alkyl and succinimidyl benzoates

A. Schaz[a]; E. Valaityte[a]; G. Lattermann[a]
[a] Makromolekulare Chemie I, Universität Bayreuth, D-95440 Bayreuth, Germany

To cite this Article Schaz, A. , Valaityte, E. and Lattermann, G.(2005) 'Investigations on liquid crystalline partially fluorinated alkyl and succinimidyl benzoates', Liquid Crystals, 32: 4, 513 — 525
To link to this Article: DOI: 10.1080/02678290412331329215
URL: http://dx.doi.org/10.1080/02678290412331329215

Liquid Crystals, Vol. 32, No. 4, April 2005, 513–525

Investigations on liquid crystalline partially fluorinated alkyl and succinimidyl benzoates

A. SCHAZ, E. VALAITYTE and G. LATTERMANN*
Makromolekulare Chemie I, Universität Bayreuth, D-95440 Bayreuth, Germany

(*Received 7 March 2003; in final form 9 March 2004; accepted 21 August 2004*)

The synthesis and mesophase properties of partially fluorinated alkoxy-substituted benzoic alkyl and succinimidyl (NHS) esters with one, two and three perfluoroalkyl alkoxy chains are reported. The mesophases were studied using differential scanning calorimetry (DSC), polarizing optical microscopy and X-ray diffraction of non-oriented samples. The SmA phases of the one-chain methyl esters are monotropic, while those of the one-chain NHS esters are enantiotropic. The more wedge-shaped two- and three-chain alkyl esters do not form mesophases, whereas the succinimidyl analogues exhibit hexagonal columnar phases. Their enhanced mesophase stability is caused by the higher polarity of the succinimidyl ring with respect to the alkyl ester groups. Aggregation of the dipolar succinimidyl groups, together with the microsegregation of the lipophilic and fluorophilic segments of the partially fluorinated alkoxy chains, is assumed to lead to a threefold structured morphology in both the SmA and the Col_h phases. This threefold structuring can be regarded as analogous to known morphologies of ABC triblock copolymers.

1. Introduction

Since the early 1980s, compounds with perfluoroalkyl chains have found increasing interest in liquid crystal research. This is due to their special properties such as enhanced chemical, thermal and mesomorphic stability and lower viscosity [1–4]. Furthermore, microsegregation between the fluorinated and non-fluorinated segments favours the tendency to form smectic phases [1, 5] and also, in the case of matching peripheral space filling, to columnar or cubic phases [6–11]; even new morphologies have been found [12]. The space filling, necessary for the curved surfaces of columnar or cubic phases, may be achieved in general by wedge-shaped molecular structures, caused by an increasing number of terminal chains, for example, going from 4-alkoxy (one-chain) benzoic acid derivatives to the corresponding 3,4-dialkoxy (two-chain) and 3,4,5-trialkoxy (three-chain) benzoic acid derivatives [13–16]. Here, we report investigations of partially fluorinated one-, two- and three-chain alkyl and succinimidyl benzoates and their mesomorphic behaviour.

2. Synthesis

In the first step, the perfluoroalkylalkoxybenzoic alkyl esters were synthesized and characterized, i.e. the methyl esters of the one-chain and three-chain compounds, **K1E[*n*,*m*]** and **K3E[*n*,*m*]**, and the ethyl esters of the two-chain compounds, **K2E[*n*,*m*]**. After hydrolysis, the corresponding acids **K*x*S[*n*,*m*]** were obtained. Finally, these were reacted with *N*-hydroxysuccinimide (NHS), to yield the *N*-succinimidyl benzoic esters **K*x*NS[*n*,*m*]**. Our acronyms are derived from the type of the compound (methyl/ethyl ester: **E**, succinimidyl ester: **NS**, acid: **S**), the number of the chains (**K1**, **K2** and **K3**, in general **K*x***) and the chain length (**[*n*,*m*]**, with *n*,*m* as the number of CF_2 and CH_2 groups, respectively).

The synthesis of the alkyl esters and of the corresponding acids largely followed the route described by Nguyen *et al.* [2] with slight modification (figure 1). After the synthesis of the ω-alkenyloxy-substituted benzoic esters with varying alkenyl chain length, *m*, via a potassium carbonate-induced etherification, perfluoroalkyl iodides of different chain length *n* were added to the terminal double bond by means of a radical chain reaction [17]. We mainly used AIBN [18] as the initiator for the radical chain, but, in a few cases used $(Ph_3P)_4Pd(0)$ [8]. The addition was followed by reductive elimination of the iodine by Bu_3SnH [18–20]. Finally, the resulting alkyl esters **K*x*E[*n*,*m*]** were hydrolysed to yield the acids **K1S[*n*,*m*]**. Then, the one-, two- and three-chain acids **K*x*S[*n*,*m*]** ($x=1$, 2, 3) were converted to the corresponding succinimidyl esters **K*x*NS[*n*,*m*]** by an esterification in the presence of *N*,*N*′-dicyclohexyl carbodiimide (DCC)

*Corresponding author.
Email: guenter.lattermann@uni-bayreuth.de

Liquid Crystals
ISSN 0267-8292 print/ISSN 1366-5855 online © 2005 Taylor & Francis Group Ltd
http://www.tandf.co.uk/journals
DOI: 10.1080/02678290412331329215

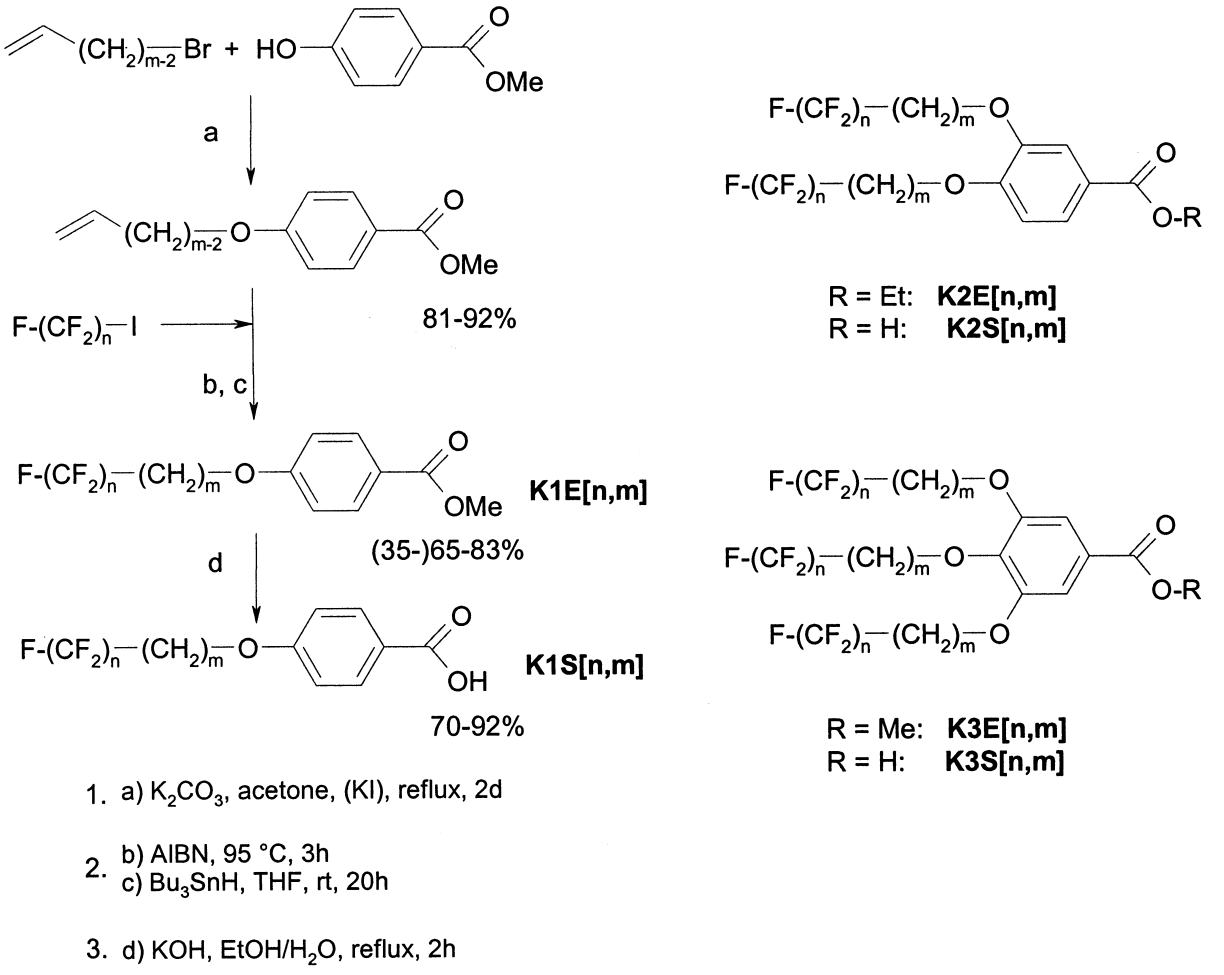

Figure 1. Synthesis of the partially fluorinated alkoxybenzoic esters and acids.

and *N*,*N*-dimethyl-4-aminopyridine (DMAP) under inert conditions [21] (figure 2). Typically, all these syntheses resulted in white compounds in acceptable to high yields (60 to over 90%).

3. Results

In this paper, the properties of the esters **K*x*E** and **K*x*NS** are reported. The investigations of the acids **K*x*S** will be discussed in further papers [22, 23]. The thermal

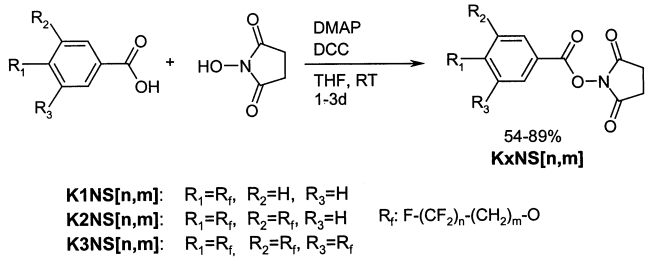

Figure 2. Synthesis of the partially fluorinated NHS esters.

behaviour of the compounds was investigated by polarizing optical microscopy (POM) and additionally, in the case of liquid crystallinity, by differential scanning calorimetry (DSC) and X-ray diffraction (XRD) of non-oriented samples.

Thermal data for the esters **K1E** are collected in table 1. Data from analogous, compounds reported in the literature (**K1E**, [5, 7, 9, 24, 25]) have been included for comparison. In the case of the new one-chain esters **K1E**, liquid crystallinity was observed in only two cases: specifically, monotropic SmA phases were seen for **K1E[10,5]** and **K1E[8,5]**. From the three-dimensional bar diagram representation of the dependence of the transition temperatures on the perfluoroalkyl chain length n and the alkyl chain length m, it may be concluded that only for $m<6$ do smectic phases exist.

In the two- and the three-chain esters **K2E** and **K3E**, no liquid crystalline behaviour was observed. In two cases, **K3E[8,11]** and **K3E[10,11]**, double melting behaviour was identified, such that the compounds

Table 1. Transition temperatures T and associated enthalpies ΔH for the one-chain methyl esters **K1E[*n*,*m*]**.

n,*m*	Cr	T/°C (ΔH/kJ mol^{-1})	SmA	T/°C (ΔH/kJ mol^{-1})	I	Ref.
6,4	•	54.0 (6.5)	•	58.0 (1.4)	•	[10, 26]
6,5	•	58.0 (36.3)	—	—	•	
6,8	•	59.5 (35.3)	—	—	•	
8,2	•	86.0 (41.3)	•	[84.0 (5.6)][b]	•	[6, 25]
8,4	•	69.0 (6.4)	•	81.0 (1.5)	•	[8, 26]
8,5	•	73.0 (41.7)	•	[71.0 (4.3)][b]	•	
8,8	•	69[a]	—	—	•	
8,11	•	75[a]	—	—	•	
10,2	•	109.0 (51.5)	•	[103.0 (6.6)][b]	•	[6, 25]
10,5	•	93.5 (39.6)	•	[90.5 (4.4)][b]	•	
10,8	•	98.5 (51.4)	—	—	•	

[a]Data from polarizing microscopy.
[b]Monotropic phase.

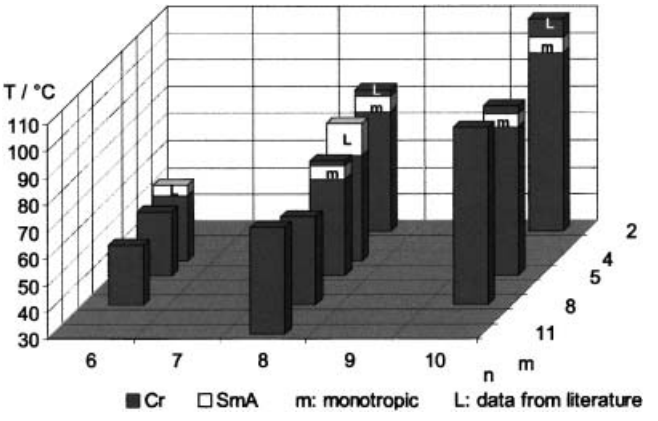

Figure 3. 3D bar diagram representing the thermal behaviour of one-chain methyl esters **K1E** (cf. table 1). SmA phases 'within' crystalline phases are monotropic; *n*,*m* is the length of the perfluoroalkyl and alkyl chains, respectively.

recrystallized from the isotropic state on heating after the first melting.

All the synthesized NHS esters **K*x*NS** show liquid crystalline phases, either SmA (**K1NS**) or Col_h phases (**K2NS** and **K3NS**). The thermal behaviour is summarized in table 2 and graphically represented in figure 4.

From the bar diagrams one can easily see that for all one-, two- and three-chain compounds, an increasing fluoro content (increasing *n*) leads to higher transition temperatures; thus, the melting points are shifted by about 20°C to higher temperatures with *n* increasing by 2. This dependency is already reported in the literature [2, 8, 26]. The effect results mainly from the greater crystallization tendency of longer perfluoroalkyl chains. For the succinimidyl esters **K*x*NS** two further relationships may be clearly detected (figure 4). First, the transition temperatures decrease strongly with increasing chain number (in the order **K1NS**, **K2NS**, **K3NS**). This may be explained by a decreasing crystallization tendency of the compounds containing the more flexible alkyl chains. Second, increasing the perfluoroalkyl chain length *n* enhances the thermodynamic mesophase stability, independently of chain number and mesophase type. Thus, in addition to the well known stabilization of smectic phases, columnar phases are

Table 2. Transition temperatures T and associated enthalpies ΔH for the NHS esters **K*x*NS[*n*,*m*]**.

x	*n*,*m*	Cr	T/°C (ΔH/kJ mol^{-1})	SmA	Col_h	T/°C (ΔH/kJ mol^{-1})	I
1	8,11	•	130.5 (48.7)	•	—	[130.0 (0.8)][a]	•
	10,5	•	153.5 (48.2)	•	—	171.5 (1.2)	•
2	6,11	•	97.5 (53.3)	—	•	117.0 (1.4)	•
	8,11	•	118.5 (59.2)	—	•	140.0 (1.6)	•
3	6,11	•	83.5 (5.7)	—	•	[74.0 (0.5)][a]	•
	8,11	•	93.5 (64.2)	—	•	99.5 (1.6)	•
	10,11	•	113.0 (78.0)	—	•	120.5 (2.1)	•

[a]Monotropic phase.

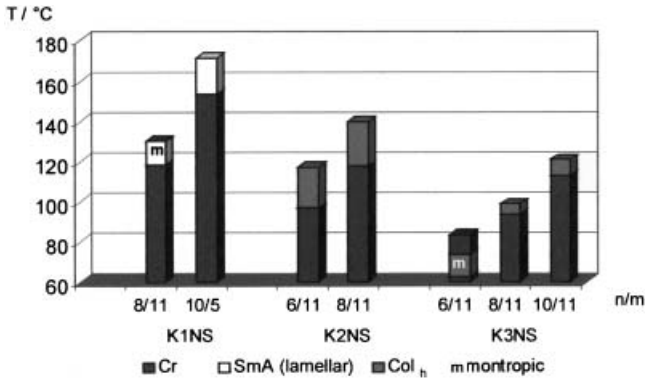

Figure 4. Diagramatic representation of the mesomorphic behaviour of the active esters **K*x*NS** (cf. table 2).

also stabilized by perfluoroalkyl chains, as previously described in the literature [7, 27].

The mesophases were identified on the basis of their optical textures (figure 5) and their X-ray diffraction patterns (figure 6). For the SmA phases (**K1E** and **K1NS**), a characteristic focal-conic fan-shaped texture was seen, figure 5 (*a*), but generally a homeotropic orientation was observed figure 5 (*b*). The latter indicates an arrangement of the optical axes perpendicular to the glass surface due to the weak interaction between the perfluoroalkyl chains and the substrate. The diffraction patterns of figures 6 (*a*,*b*) exhibit equidistant reflections. Due to the metastable behaviour of the monotropic SmA phase of the one-chain methyl esters **K1E**, only measurements in the small angle region could be performed.

The two- and three-chain NHS esters form a Col_h phase of the *P*6*mm* space group. Under POM a well developed spheroidic texture, figure 5 (*c*), appeared. The X-ray measurements reveal reflections with the relative lattice distances d_{hk0} $1 : 1/\sqrt{3} : 1/2$, indicative of Col_h phases. The X-ray data of all the mesophases are summarized in table 3.

4. Discussion

The non-fluorinated esters of 4-alkoxy-, 3,4-dialkoxy- and 3,4,5-trialkoxy-benzoic acids (i.e. the methyl and ethyl esters [28]), as well as the succinimidyl esters [15, 16, 29], are not liquid crystalline. However, introducing perfluoroalkyl chains with their strong tendencies to microsegregate from other parts of the molecules, leads to liquid crystalline behaviour. Whereas only the one-chain compounds of the relevant alkyl esters are mesogenic (SmA phases, mainly monotropic, cf. table 1), all NHS esters show liquid crystalline phases (SmA and Col_h phases, mainly enantiotropic, cf. table 2). Thus in addition to the perfluoroalkyl chains,

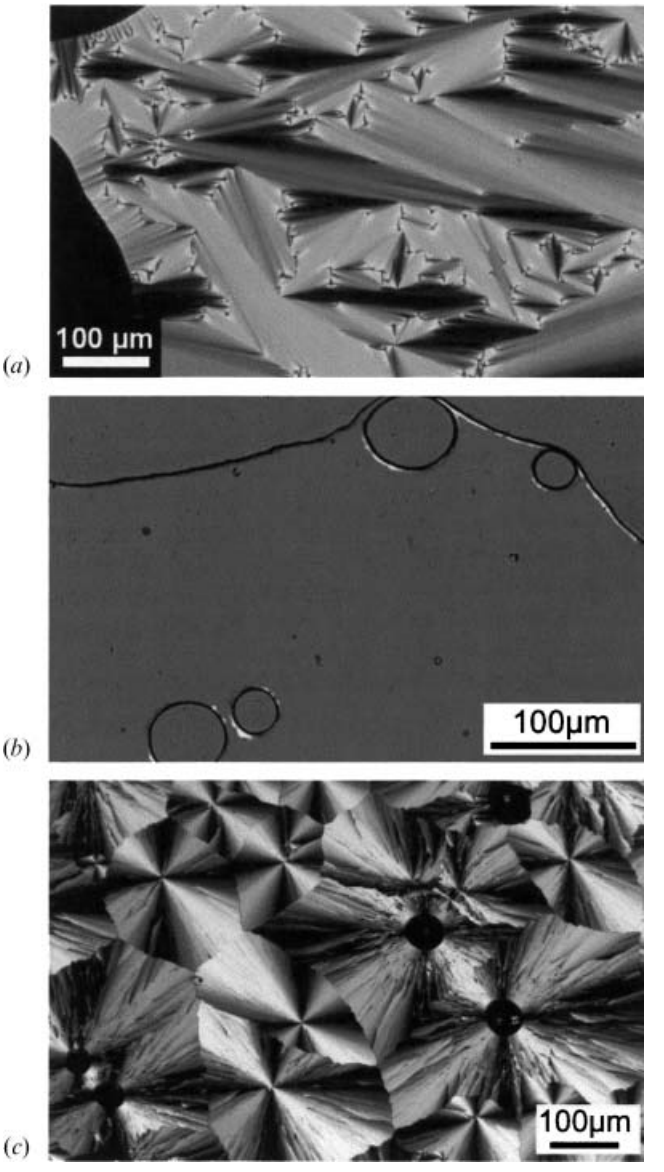

Figure 5. Typical optical textures obtained after slow cooling from the isotropic phase: (*a*) focal-conic fan-shaped texture of the monotropic SmA phase of **K1E[8,5]**, 70°C; (*b*) homeotropic orientation in the SmA phase of **K1NS[10,5]**, 170°C; (*c*) spheroidic texture of the Col_h phase of **K2NS[8,11]**, 140°C.

the type of the ester moiety also has an influence on the thermodynamic stability of the liquid crystalline phases observed.

As the increase in volume from methyl to longer alkyl chains in the ester group does not affect the thermodynamic mesophase stability remarkably [24, 30], the main stabilization factor of the NHS ester group is the higher polarity of the succinimidyl ring in **K*x*NS** with respect to the alkyl chains in **K*x*E**.

From modelling the SmA phases of the methyl esters **K1E**, we arrive at an arrangement already known in the

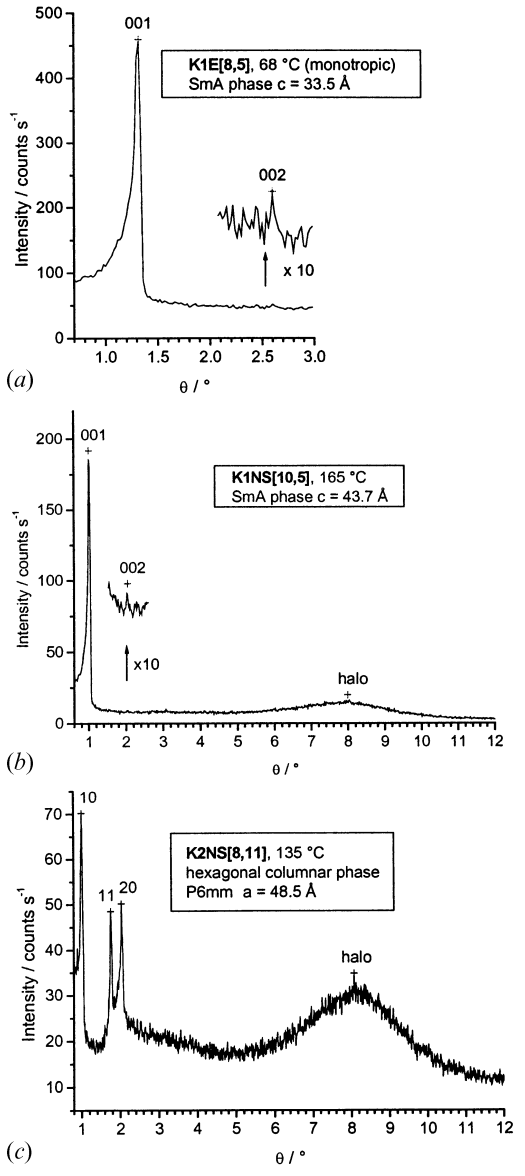

Figure 6. Typical X-ray diffraction patterns: (*a*) small angle region of the SmA phase of the methyl ester **K1E[8,5]**; (*b*) SmA phase of the succinimidyl ester **K1NS[10,5]**; (*c*) Col_h phase of the succinimidyl ester **K2NS[8,11]**.

literature [31]. The perfluoroalkyl chains are arranged parallel in one layer, while the alkyl chains, the benzoic ring and the ester moiety interdigitate in the second layer (figure 7). This is presumably due to the microsegregation between perfluoroalkyl chains and the rest of the molecule. In this case, the layer thickness L is the sum of twice the length of the perfluoroalkyl segment and the length of the non-fluorinated part; or, in other words, the sum of one whole molecular length l_{Mol} and one perfluoroalkyl segment l_F: $L=l_{Mol}+l_F$. From molecular modelling we were able to calculate these dimensions and to compare them with the measured layer constant c. The results are given in table 4.

Because of the elongated all-*trans* alkyl chains in the molecular modelling calculation, the calculated layer thickness L is somewhat larger than the measured layer distance c. Taking into account the *gauche* defects in molten alkyl chains which reduces the molecular length, the L-values have to be similarly reduced, such that they are close to the measured lattice distances c. In figure 7, the molecules are arranged with molten alkyl chains instead of all-*trans* conformations. According to the c- and L-values in table 4, the reduced length of the molten pentyl chains ($m=5$) with respect to their extended conformation $(L\text{-}c)/L$ is always nearly 7%.

As concluded previously, the main thermodynamic stabilization effect of the succinimidyl ring in **K1NS** on the mesomorphism is its higher polarity with respect to the alkyl ester moiety in **K1E**. Presumably, the molecules minimize their dipole interactions via antiparallel dipole correlations. This is only possible if the succinimidyl rings are located within their own sublayer. This correlation is similar to the arrangement of, for example, polar *para*-CN-substituted compounds in their smectic phases [32]. Therefore, the molecules are assumed to form the layered structure shown in figure 8.

According to this model with a CBABC sequence, L is now the sum of twice the length of the perfluoroalkyl chain, twice that of the alkyl chain and the length of the ring system; or, in other words, the molecular length l_{Mol} plus the alkyl chain length l_H plus the perfluoroalkyl chain length l_F: $L=l_{Mol}+l_H+l_F$ (table 5). The calculation of the reduced alkyl chain length with respect to the extended alkyl chain (here: $[(L\text{-}c)/L]/2$) confirms this three-fold layered arrangement. With pentyl chains ($m=5$), the reduction amounts to about 7.3%, which fits well with the reduction of nearly 7% in **K1E** (cf. table 4). The assumption of a layering as seen in the models of the **K1E** in figure 7, would give a reduction of only 3.3% per molten alkyl chain instead, with $L=l_{Mol}+l_F$ and $(L\text{-}c)/L$ for the reduced length. The reduction of 12.5% in **K1NS[8,11]** is apparently due to the longer alkyl chain ($m=11$).

To establish a structural model of the columnar phases of the two- and three-chain active esters **K2NS** and **K3NS**, we calculated in two ways the number of molecules N per lattice element, which is equivalent to its unit cell for a hexagonal lattice N. The number of molecules per lattice element (unit cell) N_M, according to the first method, is related to the molecular mass M, which is compared with the mass of the unit cell m_E, as shown in equation (1). The mass of all molecules in the unit cell is given by equation (2). The density ρ has been

Table 3. X-ray data of all the mesophases of the compounds synthesized. *n,m*=length of the perfluoroalkyl and the alkyl chain; *T*=measurement temperature; θ=diffraction angle.

Compound	*n,m*	Phase	*T*/°C	Lattice parameter/Å	θ/° measured calculated
					hkl 001/002
K1E	8,5	SmA[a]	65	*c*=33.5	1.32/2.63
				halo: —[b]	*1.32/2.64*
	10,5	SmA[a]	90	*c*=38.5	1.15/2.28
				halo: —[b]	*1.15/2.29*
K1NS	8,11	SmA[a]	130	*c*=46.7	0.95/1.88
				halo: 5.3	*0.95/1.89*
	10,5	SmA	165	*c*=43.2	1.01/2.05
				halo: 5.5	*1.02/2.04*
					hkl: 10/11/20/21
K2NS	6,11	Col_h	110	*a*=48.4	1.05/1.82/2.12/—
				halo: 5.3	*1.05/1.82/2.11*
	8,11	Col_h	135	*a*=50.2	1.01/1.76/2.03/—
				halo: 5.5	*1.02/1.76/2.03*
K3NS	6,11	Col_h[a]	70	*a*=45.1	1.13/1.96/2.29/—
				halo: 5.1	*1.13/1.96/2.26*
	8,11	Col_h	90	*a*=47.6	1.07/1.85/2.14/2.83
				halo: 5.3	*1.07/1.85/2.14/2.83*
	10,11	Col_h	117	*a*=50.0	1.02/1.76/2.05/—
				halo: 5.4	*1.02/1.77/2.04*

[a]Monotropic phase.
[b]Measurement only in the small angle region.

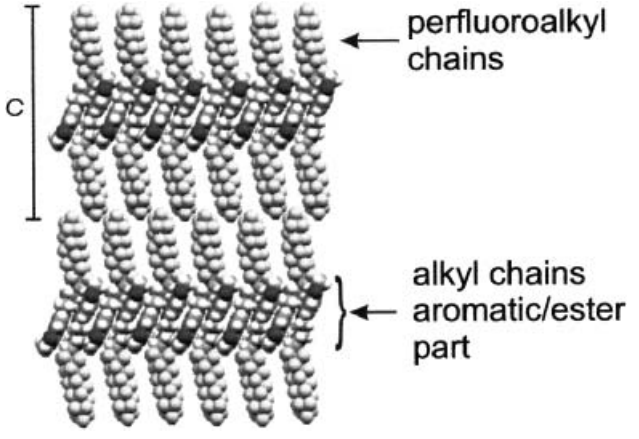

Figure 7. Model of the SmA phase of the one-chain methyl esters **K1E**.

generally set to 1 g cm^{-3}: density measurements with **K2S[8,11]** revealed this value. The unit cell volume V_E was calculated according to equation (4), with the lattice constant *a* taken from the X-ray measurements (cf. table 3) and with *c*=4 Å for the intercolumnar distance of the molecules. This value of *c* is an average between

Table 4. Modelling of the SmA phases of the one-chain methyl esters **K1E**. *c*=measured lattice parameter (layer period); l_F, l_{Mol}=length of the perfluoroalkyl chain and of the entire molecule, resp., obtained by molecular modelling; *L*=resulting layer thickness, if overlapping of the non-fluorinated part is assumed, $L=l_{Mol}+l_F$.

n,m	*c*/Å	l_F/Å	l_{Mol}/Å	*L*/Å	$\frac{L-c}{L}\times 100$
8,5	33.5	10.3	25.9	36.0	6.9
10,5	38.5	12.7	28.5	41.2	6.6

Table 5. Modelling of the SmA phases of the one-chain succinimidyl esters **K1NS**. *c*=measured lattice parameter (layer period); l_H, l_F, l_{Mol}=length of the alkyl chain, the perfluoroalkyl chain and the entire molecule, resp., obtained by molecular modelling; *L*=resulting layer thickness, if overlapping of the aromatic/succinimicyl part is assumed, $L=l_{Mol}+l_H+l_F$.

n,m	*c*/Å	l_F/Å	l_H/Å	l_{Mol}/Å	*L*/Å	$\frac{L-c}{2L}\times 100$
8,11	46.7	10.3	14.0	38.0	62.3	12.5
10,5	43.2	12.7	6.3	31.6	50.6	7.3

Table 6. Number of molecules N in the Col_h phases of the two- and three-chain succinimidyl esters **K2NS** and **K3NS**. a=lattice constant from X-ray measurements, N_M, $N_{\Delta V}$=calculated number of molecules per lattice element (elemental cell)—N_M via the molecular mass M and the density ρ, $N_{\Delta V}$ via volume increments. N=rounded up average of N_M and $N_{\Delta V}$.

Compound	*n*,*m*	Phase	*a*/Å	M/g mol^{-1}	N_M	V_{Mol}/Å^3	$N_{\Delta V}$	N
K2NS	6,11	Col_h	48.4	1195	4.1	975	4.6	4
	8,11	Col_h	50.2	1395	3.8	1104	4.3	4
K3NS	6,11	Col_h	45.1	1683	2.5	1376	2.8	2
	8,11	Col_h	47.6	1983	2.4	1570	2.8	2
	10,11	Col_h	50.0	2283	2.3	1764	2.7	2

the mean distance of alkyl moieties of 3.3 Å and the mean distance of perfluoroalkyl chains of 5 Å.

To verify these calculations, in the second method we estimated the molecular volume V_{Mol} via volume increments of the different groups in the molecule according to Kitaigorodsky [33]. Corrected by the packing parameter k=0.55, which takes into account the free volume in a condensed phase [33], the resulting volume V_{Mol}/k is set in relation to the cell volume V_E, leading to the number of molecules per unit cell $N_{\Delta V}$ (equation 3). The average and rounded up values of N_M and $N_{\Delta V}$ result in the final number of molecules N per unit cell, as shown in table 6.

$$N_M = \frac{m_E N_A}{M} = \frac{V_E \rho N_A}{M} \quad (1)$$

$$m_E = \rho V_E \quad (2)$$

$$N_{\Delta V} = \frac{V_E}{V_{Mol}/k} \quad (3)$$

with

$$V_E = \frac{\sqrt{3}a^2}{2} c \text{ (hexagonal cell).} \quad (4)$$

For the two-chain NHS esters **K2NS**, a number of N=4 molecules per unit cell is obtained. This may correspond to two 'dimers', by analogy to the dimerization of **K1NS** in their SmA phases. Thus, the molecules of **K2NS** may arrange in the Col_h phase as shown in figure 9. For the three-chain succinimidyl esters **K3NS**, values of N=2 and N=3, are possible at a first inspection, according to N_M and $N_{\Delta V}$. However for N=2, the modelled unit cell shows too much free space whereas for N=3 acceptable space filling results. Thus, we concluded the latter value to be more realistic.

Comparison of the stability and structure of the mesophases of NHS esters **K*x*NS** with respect to alkyl esters **K*x*E** leads to a schematic structure of strongly segregated molecular subunits, as shown in figures 8

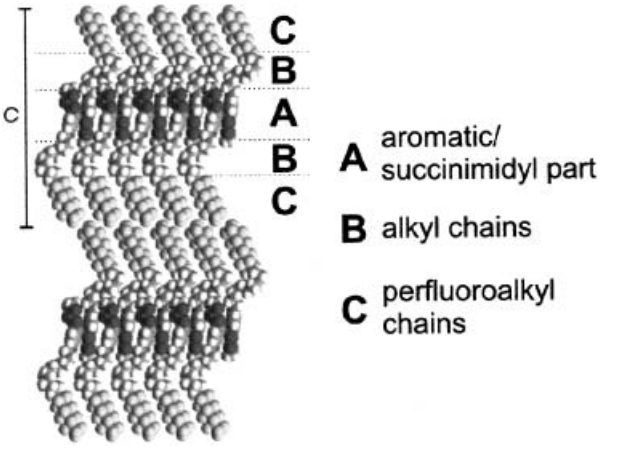

Figure 8. Model of the SmA phase of the one-chain succinimidyl ester **K1NS**.

and 9. Here, CBABC sequences of the segregated molecular parts are present, resulting from ABC mesogens, as schematically shown in figure 10. In consequence, these microsegregated phases of low molar mass compounds may be regarded as being analogous to phases of microphase-separated ABC triblock copolymers.

5. Conclusion

The succinimidyl esters **K*x*NS** are examples of partially fluorinated mesogens showing smectic and columnar mesophases. With respect to the alkyl esters **K*x*E**, the increasing polarity in the ester moiety from methyl/ethyl groups to the succinimidyl ring leads to a strong thermodynamic stabilization of SmA phases (one-chain compounds) or to the formation of columnar phases (two- and three-chain compounds). This stabilization effect may be explained by the formation of 'dimers' due to the strong dipolar character of the succinimidyl moiety. This dimerization may thus be compared with the H-bond dimers of mesomorphic alkylated benzoic acids. The second driving force for the reported mesophase formation is microsegregation due to the

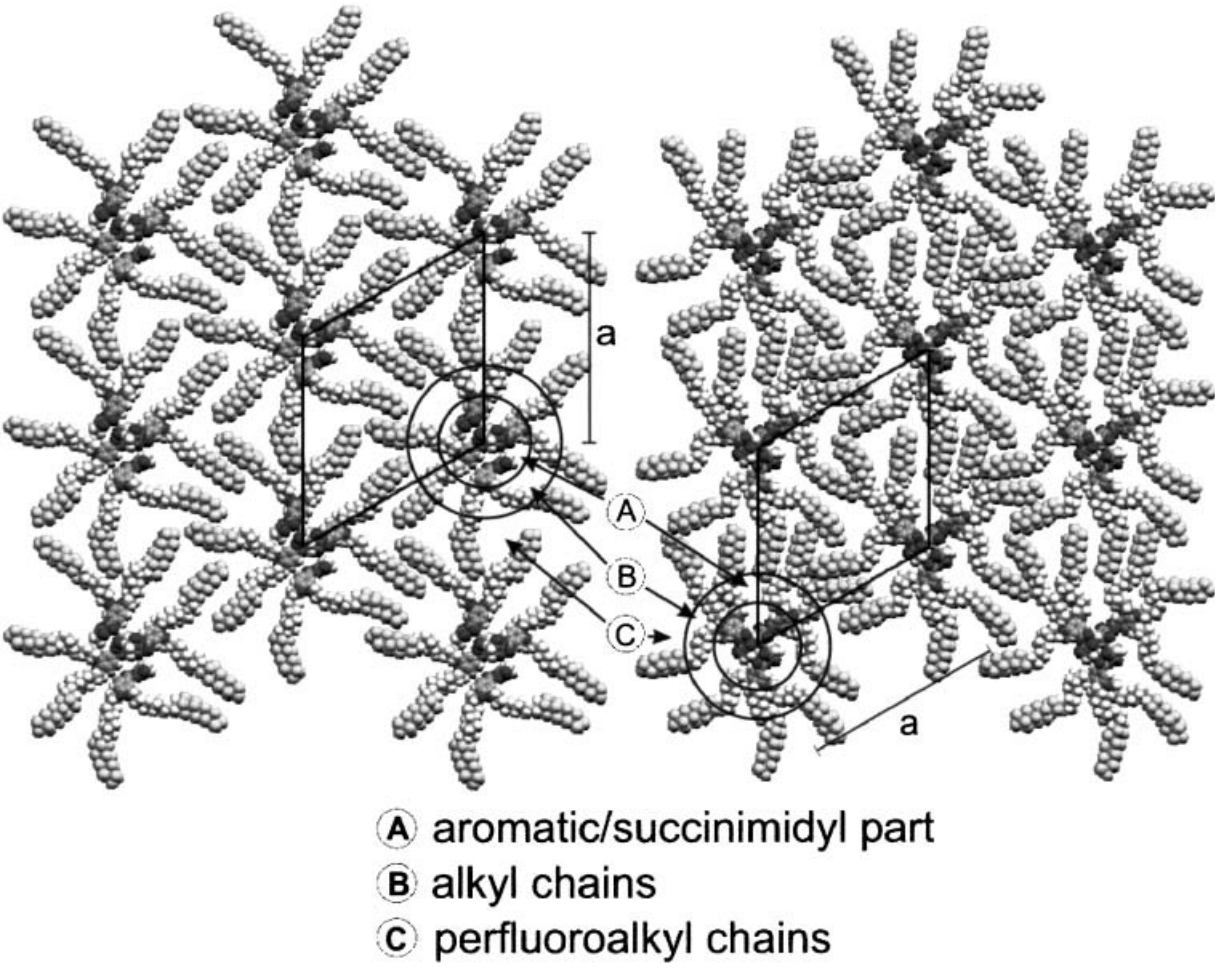

Figure 9. Formation of aggregates of the two- and three-chain NHS esters **K2NS** (left) and **K3NS** (right).

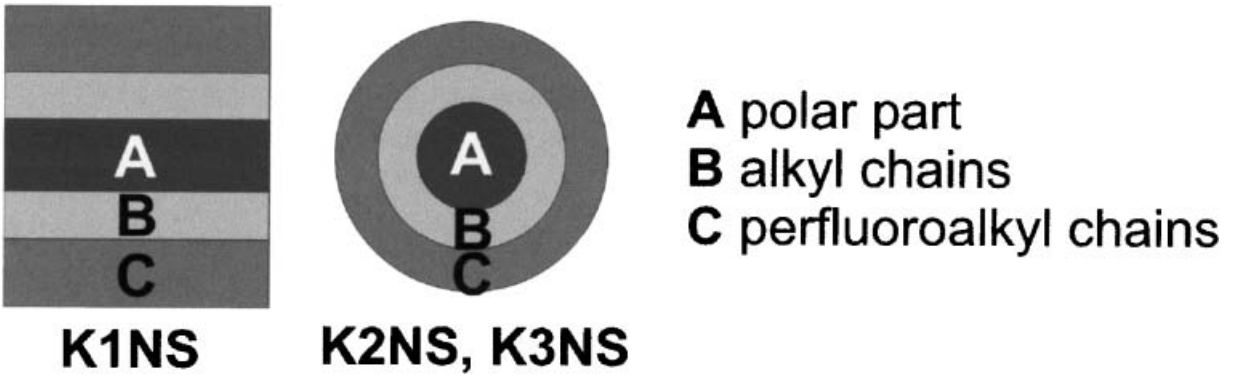

Figure 10. Schematic ABC morphology of the SmA and the Col_h phases of the NHS esters **K*x*NS**.

incompatibility of the perfluoroalkyl chains with the rest of the molecules. The non-fluorinated esters (methyl, ethyl and succinimidyl) form no mesophases.

The presence of three distinct parts in the molecules (perfluoroalkyl chains, alkyl chains, succinimidyl ring), together with aggregation of the succinimidyl ring and microsegregation, leads to the proposed mesophase structures of ABC mesogens analogous to the phases of ABC triblock copolymers.

6. Experimental

6.1. *Characterization*

Infrared spectra were recorded with a Bio-Rad FTS 40 FTIR spectrometer at a resolution of $4\,cm^{-1}$. Pellets of 1 mg of compound, dispersed in 100 mg of KBr for solids, or films of the liquids, between two pellets of pure KBr, were used. NMR spectra of solutions in chloroform-*d*, with some trifluoroacetic acid-*d* were measured on a Bruker AC 250 spectrometer (250 MHz for ^{1}H, 62.5 MHz for ^{13}C). Chemical shifts are given in ppm relative to TMS (tetramethyl silane) as internal standard.

TLC was performed on precoated slides with silica gel and a fluorescence indicator, purchased from Macherey & Nagel. The spots were detected by UV and staining with iodine vapour. Size exclusion chromatography (SEC) was performed using two 600×8 mm columns, filled with polystyrene gel (5 µm particle size, 500 Å and 100 Å pore size, Polymer Laboratories). The eluant was THF at $0.5\,ml\,min^{-1}$. Chromatograms were registered using a Waters 440 absorbance detector at 245 nm and a Waters 410 differential refractometer at 30°C. Gas chromatography was performed on a Chrompack gaschromatograph CP9000 at 40°C.

Thermal analysis was carried out using a Perkin Elmer DSC 7 apparatus at a heating rate of $10^{\circ}C\,min^{-1}$. Polarising microscopy was performed on a Nikon Diaphot 300, equipped with hot stage Mettler FP82. Photographs were taken with a Nikon F4 camera.

X-ray measurements were recorded on a Guinier diffractometer ($CuK_{\alpha 1}$ irradiation, $\lambda = 1.54051$ Å, quartz monochromator) with scintillation counter, home-made heating device (accuracy of $\pm 0.5^{\circ}C$) and computer control. Electron impact mass spectrometry (EI-MS) was provided by the Central Analytical Department of Universität Bayreuth using a Finnigan MAT 8500; MAT 112 S from Varian.

Elemental analyses were provided by the Micro-analytical Laboratory of the Technische Universität München. Results for fluorine may be low. For density measurement, a molten sample was cooled and brought into water. Ethanol was added continuously, until the sample started to sink. The density of the liquid was then measured by weighing a 10 ml sample of the ethanol/water mixture.

6.2. *Materials*

Argon was dried and purified first over molecular sieve (3 Å) and then by passing through a column filled with potassium dispersed on neutral alumina. THF was distilled over potassium; pentane was purified by distillation from sodium/potassium alloy. All other solvents were distilled through a 300 mm Vigreux column.

Perfluoroalkyl iodides (gift from Clariant) were received as a mixture of the homologues ($n = 6$, 8, 10, 12, 14). To obtain the pure compounds, a fractional distillation under reduced pressure was performed (300 to 10 mbar, depending on n). Finally, the liquid perfluoroalkyl iodides were washed with aqueous sodium thiosulphate solution; solid products were recrystallized from toluene to remove free iodine. The pure compounds were stored at $-18^{\circ}C$. 5-Bromo-1-pentene, 8-bromo-1-octene and 11-bromo-1-undecene were synthesized as previously described [34]. Azoisobutyronitrile (AIBN, Merck) was recrystallized from methanol below 40°C; *N*,*N*-dimethyl-4-aminopyridine (DMAP, Merck) was recrystallized several times from acetone and dried *in vacuo*. All other reagents were commercially available (Aldrich, Merck, Fluka, Avocado) and used as received.

The main problems in all the synthesis reactions were the strongly different solubilities of the fluorinated compounds and their tendency to form foams during work-up. The solvents had always to be adapted to the compounds used; foams could be depressed in the rotatory evaporator using rather high temperatures of the water bath. Another problem with compounds having longer perfluoroalkyl chains is their invisibility on TLC sheets (UV detection, iodine staining). Other methods such as NMR or SEC had to be used for purity control. Finally, the compounds normally do not crystallize well, forming gel-like precipitates during purification.

6.2.1. Alkenylbenzoates

6.2.1.1. *Methyl 4-(ω-alkenyloxy)benzoates*

One equivalent (about 65 mmol) of ω-bromo-1-alkene and 1.1 equiv. of methyl 4-hydroxybenzoate were dissolved in 200 ml acetone. Potassium carbonate (5 equiv.) and potassium iodide (0.1 equiv.) were added and the suspension was heated under reflux. The reaction was monitored by TLC (cyclohexane/ethyl acetate = 5/1). As soon as the bromo compound was no longer detectable (after about 2 days), the solids were

filtered off and the solvent evaporated. The crude products were either recrystallized from ethanol (solids) or distilled under reduced pressure (liquids). Yields and R_f (cyclohexane/ethyl acetate): m=5: 90%, R_f (9/1)= 0.52; m=8: 81%, R_f (5/1)=0.68; m=11: 92%, R_f (5/1)= 0.66. Example of spectral data, for methyl 4-(4-pentenyloxy)benzoate: IR (film): ν/cm^{-1}=2951, 2878, 1718, 1607, 1512, 1436, 1282, 1255, 1170, 848, 771. ^{1}H NMR: δ (ppm)=1.90 (m, 2H, CH_2–CH_2–O), 2.25 (qa, [7.2 Hz], 2H, CH_2–CH), 3.88 (s, 3H, OCH_3), 4.01 (t, [6.4 Hz], 2H, CH_2–O), 5.03 (m, HCH=CH, *cis*), 5.05 (m, HCH=CH, *trans*), 5.85 (m, H_2C=CH), 6.90 (d, [8.7 Hz], 2 H_{ar}*ortho* to C–O–CH_2), 7.98 (d, [8.7 Hz], 2 H_{ar}*ortho* to C–COOMe). ^{13}C NMR: δ (ppm)=28.2/30.0 ((*C*H_2)$_2$–CH), 51.8 (O–*C*H_3), 67.3 (*C*H_2–O), 114.0 (H_2C=CH), 115.3 (C_{ar} *ortho* to C–O), 122.3 (*C*–CO), 131.5 (C_{ar}*ortho* to C–CO), 137.5 (H_2C=*C*H), 162.8 (CH_2–O–*C*), 166.9 (*C*=O).

6.2.1.2. *Ethyl 3,4-di(ω-alkenyloxy)benzoates*

The same procedure as for the one-chain compounds was used, with about 55 mmol (one equiv.) of ethyl 3,4-dihydroxybenzoate and 2.2 equiv. of the bromo compound. Variation: as soon as no hydroxy compound was detectable by TLC, another 0.2 equiv. of ethyl 3,4-dihydroxybenzoate was added in order to remove surplus bromo compound. After a further 2 days of reaction time, the solids were filtered off and the solvent evaporated. The crude oil was dissolved in diethyl ether and the solution filtered over a column of basic alumina; the solvent was finally evaporated. Yields and R_f (cyclohexane/ethyl acetate): m=8: 94%, R_f (5/1)=0.68; m=11: 86%, R_f (9/1)=0.57. Example of spectral data, for ethyl 3,4-di-(7-octenyloxy)benzoate: IR (film): ν/cm^{-1}=3077, 2977, 2930, 2857, 1714, 1640, 1600, 1513, 1466, 1430, 1270, 1214, 1132, 1105, 1026, 909, 764, 645. ^{1}H NMR: δ (ppm)=1.3–1.6 (m, 15H, (CH_2)$_3$–C_2H_4–O, CH_3), 1.84 (m, 4H, CH_2–CH_2–O), 2.05 (qa, [6.4 Hz], 4H, CH_2–CH), 4.04 (t, [6.6 Hz], 4H, CH_2–O), 4.34 (qa, [7.1 Hz], 2H, O–CH_2–CH_3), 4.94/4.99 (m, 4H, H_2C=CH), 5.81 (m, 2H, H_2C=CH), 6.86 (d, [6.2 Hz], 1 H_{ar}), 7.54 (d, [2.0 Hz], 1 H_{ar}), 7.64 (dd, [6.2 Hz, 2.0 Hz], 1 H_{ar}).

6.2.1.3. *Methyl 3,4,5-tri(ω-alkenyloxy)benzoates*

The same procedure as for the two-chain compounds was used, with about 40 mmol (one equiv.) of methyl 3,4,5-trihydroxybenzoate and 3.3 equiv. of the bromo compound. Yields and R_f (cyclohexane/ethyl acetate): m=8: 97%, R_f (5/1)=0.77; m=11: 90%, R_f (9/1)=0.73. Example of spectral data, for methyl 3,4,5-tri(7-octenyloxy)benzoate: IR (film): ν/cm^{-1}=3079, 2930, 2856, 1722, 1641, 1587, 1500, 1433, 1336, 1218, 1118, 1016, 909, 766. ^{1}H NMR: δ (ppm)=1.3–1.6 (m, 18H, (CH_2)$_3$–C_2H_4–O), 1.7–1.9 (m, 6H, CH_2–CH_2–O), 2.06 (qa, [6.7 Hz], 6H, CH_2–CH), 3.89 (s, 3H, OCH_3), 4.01 (t, [6.6 Hz], 6H, CH_2–O), 4.94/4.99 (m, 6H, H_2C=CH), 5.82 (m, 3H, H_2C=CH), 7.25 (s, 2 H_{ar}).

6.2.2. Perfluoroalkylalkyloxybenzoates

6.2.2.1. *Methyl 4-(perfluoroalkylalkoxy)benzoates* ***K1E***

About 12 mmol (one equiv.) of the corresponding methyl 4-(ω-alkenyloxy)benzoate were mixed with 1.1 equiv. of the perfluoroalkyl iodide. At room temperature or slightly elevated, the liquid mixture was degassed by passing through it a small inert gas flow for 30 min. The temperature was then raised to 90°C and several small portions of AIBN (each about 0.01 equiv.) were added over 1 h. The temperature was then raised to 100°C and a further 0.1 equiv. of AIBN added. The reaction was monitored by TLC (CH_2Cl_2/cyclohexane=2/1). After completion of the reaction, the mixture was cooled to room temperature and dissolved in 10–30 ml THF, depending on the solubility. Bu_3SnH (2.2 equiv.) was added and the solution stirred for 20 h. The temperature was raised to 45°C and the mixture stirred for another 2 h; the solvent was evaporated and the product recrystallized several times from methanol (n=6) or ethanol (n=8, 10). Yields and R_f (CH_2Cl_2/cyclohexane=2/1): **K1E[6,5]**: 83%, R_f=0.61; **K1E[6,8]**: 88%, R_f=0.60; **K1E[8,5]**: 35%, R_f=0.61; **K1E[8,8]**: 81%, R_f=0.61; **K1E[8,11]**: 65%, R_f=0.61; **K1E[10,5]**: 35%, R_f=0.59; **K1E[10,8]**: 77%, R_f=0.60. Thermal data are listed in table 1. Example of spectral data, for methyl 4-(perfluorohexylpentyloxy)benzoate **K1E[6,5]**: IR (KBr): ν/cm^{-1}=2957, 2878, 1720, 1606, 1513, 1283, 1255, 1172, 1140, 1045, 698. ^{1}H NMR: δ (ppm)=1.5–1.8 (m, 4H, (CH_2)$_2$–C_2H_4–O), 1.85 (pseudo-qi, [6.8 Hz], 2H, CH_2–CH_2–O), 2.11 (tt, [8.0 Hz, 18.8 Hz], 2H, CF_2–CH_2), 3.88 (s, 3H, OCH_3), 4.03 (t, [6.2 Hz], 2H, CH_2–O), 6.90 (d, [7.9 Hz], 2 H_{ar}*ortho* to C–O–CH_2), 7.98 (d, [8.0 Hz], 2 H_{ar}*ortho* to C–COOMe). ^{13}C NMR: δ (ppm)=19.9 (t, [3.8 Hz], *C*H_2–CH_2–CF_2), 25.6/28.7 ((*C*H_2)$_2$–CH_2–O), 30.7 (t, [21.8 Hz], CF_2–*C*H_2), 51.6 (O–*C*H_3), 67.6 (*C*H_2–O), 113.9 (C_{ar}*ortho* to C–O), 122.5 (*C*–CO), 131.5 (C_{ar}*ortho* to C–CO), 162.7 (H_2C–O–*C*), 166.8 (*C*=O).

6.2.2.2. *Ethyl 3,4-bis(perfluoroalkylalkoxy)benzoates* ***K2E***

In contrast to the one-chain esters **K1E**, the two-chain esters **K2E** were synthesized by a $(Ph_3P)_4Pd(0)$-activated addition of the perfluoroalkyl iodide to the alkenyl ester, in order to shorten the reaction time. About 5 mmol (1 equiv.) of the ethyl 3,4-di(ω-alkenyloxy)benzoate and 2.2 equiv. of the perfluoroalkyl iodide were

dissolved in 30 ml of absolute pentane under inert conditions. After addition of 4 mol% of $(Ph_3P)_4Pd(0)$, the suspension was stirred for about one week, while monitoring the reaction by TLC. After the reaction was finished, the solid product was filtered off and the solvent evaporated.

The reduction was performed in the same way as described for the one-chain esters **K1E** with 3.5 equiv. Bu_3SnH. Recrystallization media, yields, melting points and R_f (CH_2Cl_2/cyclohexane=2/1): **K2E[6,8]**: not purified, R_f=0.68; **K2E[6,11]**: EtOH at 2°C, 61%, T_m=43°C; R_f=0.68; **K2E[8,8]**: EtOH, 90%, T_m=59°C; R_f=0.66; **K2E[8,11]**: EtOH/toluene=9/1, 92%, T_m=65°C; R_f=0.66; **K2E[10,8]**: $CHCl_3$, 80%, T_m=84°C; R_f=0.68; **K2E[10,11]**: EtOH/toluene=9/1, 92%, T_m=76°C; R_f=0.68. Example of spectral data, for ethyl 3,4-bis(perfluorohexylundecyloxy)benzoate **K2E[6,11]**): IR (KBr): ν/cm^{-1}=2937, 2856, 1717, 1602, 1517, 1471, 1432, 1344, 1215, 1153, 1109, 882, 765, 647. ^{1}H NMR: δ (ppm)=1.2–1.8 (m, 39H, $(CH_2)_9$–C_2H_4–O, CH_3), 2.05 (tt, [18.8 Hz, 7.7 Hz], 4H, CH_2–CF_2), 4.04 (t, [6.4 Hz], 4H, CH_2–O), 4.34 (qa, [7.1 Hz], 2H, CH_2–CH_3), 6.86 (d, [8.5 Hz], 1 H_{ar}), 7.54 (d, [2.0 Hz], 1 H_{ar}), 7.64 (dd, [8.5 Hz, 2.0 Hz], 1 H_{ar}).

6.2.2.3. *Methyl 3,4,5-tris(perfluoroalkylalkoxy) benzoates* ***K3E***

The same procedure as for the one-chain esters **K1E** was used, with about 4 mmol (one equiv.) of methyl 3,4,5-tri(ω-alkenyloxy)benzoate, 3.3 equiv. perfluoroalkyl iodide and 5 equiv. Bu_3SnH. Recrystallization media, yields, melting points and R_f (CH_2Cl_2/cyclohexane=2/1): **K3E[6,8]**: ethyl acetate, 54%, T_m=67°C; R_f=0.75; **K3E[6,11]**: EtOH/acetone=3/1, 82%, T_m=61°C; R_f=0.75; **K3E[8,8]**: ethyl acetate, 69%, T_m=92°C; R_f=0.74; **K3E[8,11]**: acetone, 81%, T_m=64/84°C; R_f=0.74; **K3E[10,8]**: ethyl acetate, 82%, T_m=112°C; R_f=0.75; **K3E[10,11]**: EtOH/acetone=3/1, 82%, T_m=93/104°C; R_f=0.75. **K3E[8,11]** and **K3E[10,11]** show double melting behaviour, the second melting point is visible after annealing above the first melting point. Example of spectral analyses, for methyl 3,4,5-tris(perfluorohexyloctyloxy)benzoate **K3E[6,8]**): IR (KBr): ν/cm^{-1}=2944, 2859, 1726, 1589, 1471, 1439, 1249, 1211, 1145, 1122, 1051, 1000, 697, 654. ^{1}H NMR: δ (ppm)=1.3–1.7 (m, 30H, $(CH_2)_5$–C_2H_4–O), 1.82 (pseudo-qi, [7.2 Hz], 6H, CH_2–CH_2–O), 2.05 (tt, [18.4 Hz, 8.5 Hz], 6H, CH_2–CF_2), 3.89 (s, 3H, O–CH_3), 4.01 (t, [6.6 Hz], 6H, CH_2–O), 7.26 (s, 2 H_{ar}).

6.2.3. Perfluoroalkylalkoxybenzoic acids.

One equiv. (about 5 mmol) of the ester **K1E**, **K2E** or **K3E** was dissolved in 50–250 ml aqueous alcohol (ethanol/water=5/1 to isopropanol/water=20/1, depending on the solubility). After heating to reflux, 10 equiv. of KOH was added with subsequent stirring of the mixture for 3 h. The reaction mixture was they poured into ice water and acidified (pH 1) with conc. aqueous HCl. The white precipitate was filtered off and recrystallized from ethanol or ethyl acetate; yield 70–90%. Due to aggregation of the acids and interaction with the column gel, no SEC measurements were possible with these compounds. Instead, C,H elemental analyses were performed for purity check, as shown in table 7.

6.2.3.1. *4-(perfluoroalkylalkoxy)benzoic acids* ***K1S***

Example of spectral data, for 4-(perfluorohexyloctyloxy-benzoic acid **K1S[6,8]**: IR (KBr): ν/cm^{-1}=3300–2400, 2947, 2860, 2662, 2566, 1671, 1607, 1578, 1515, 1432, 1307, 1261, 1171, 1145, 848, 775, 697, 646. ^{1}H NMR: δ (ppm)=1.3–1.7 (m, 10H, $(CH_2)_5$–C_2H_4–O), 1.81 (pseudo-qi, [6.7 Hz] 2H, CH_2–CH_2–O), 2.12 (tt, [8.0 Hz, 18.6 Hz], 2H, CH_2–CF_2), 4.09 (t, [6.2 Hz], 2H, CH_2–O), 6.96 (d, [8.7 Hz], 2 H_{ar}*ortho* to C–O–CH_2), 8.05 (d, [8.7 Hz], 2 H_{ar} *ortho* to C–COOH). ^{13}C NMR: δ (ppm)=20.4 (CH_2–CH_2–CF_2), 26.2/29.2/29.3/29.4/29.4 (CH_2), 31.2 (t, [22.4 Hz], CF_2–CH_2), 68.9 (CH_2–O), 114.9/120.2/133.2/164.7 (C_{ar}), 173.1 (COOH). For mass spectroscopy and elemental analyses see table 7.

Table 7. Examples for electron impact mass spectroscopy and elemental analyses of acids **K*x*S** and NHS esters **K*x*NS**.

		Elemental analyses %		
Compound	EI-MS calc. M/g mol^{-1} (found m/z)	C calc. (found)	H calc. (found)	N calc. (found)
K1S[6,8]	568 (568)	44.38 (43.98)	3.72 (3.46)	—
K2S[8,8]	1214 (1214)	38.56 (38.35)	2.88 (2.99)	—
K3S[10,11]	2186 (2186)	38.44 (38.57)	3.18 (3.08)	—
K2NS[8,11]	1395 (1395)	42.16 (41.56)	3.68 (3.59)	1.00 (1.10)
K3NS[8,11]	1983 (1983)	41.16 (41.35)	3.66 (3.71)	0.71 (0.87)

6.2.3.2. *3,4-Bis(perfluoroalkylalkoxy)benzoic acids* ***K2S***

Example of spectral data, for 3,4-bis(perfluorooctyl-undecyloxy)benzoic acid **K2S[8,11]**: IR (KBr): ν/cm^{-1}=3400–2400, 2922, 2850, 1681, 1599, 1520, 1471, 1446, 1279, 1204, 1149, 1051, 1023, 872, 769, 722, 659. ^{1}H NMR: δ (ppm)=1.2–1.5 (m, 28H, (CH_2)$_7$–C$_2$H$_4$–O), 1.58 (pseudo-qi, [7.6 Hz] 4H, CH_2–CH$_2$–CF$_2$), 1.84 (pseudo-qi, [5.9 Hz], 4H, CH_2–CH$_2$–O), 2.04 (tt, [18.3 Hz, 8.1 Hz], 4H, CF$_2$–CH_2), 4.1–4.2 (m, 4H, CH_2–O), 6.97 (d, [8.6 Hz], 1 H_{ar}), 7.57 (d, [2.0 Hz], 1 H_{ar}), 7.70 (dd, [8.5 Hz, 2.0 Hz], 1 H_{ar}). ^{13}C NMR: δ (ppm)=20.4 (*C*H$_2$–CH$_2$–CF$_2$), 26.0/28.9–29.8/30.0 ((CH$_2$)$_8$–CH$_2$–O), 31.2 (t, [22.7 Hz], CF$_2$–CH$_2$), 70.2, 71.2 (CH$_2$–O), 112.6/116.3/120.6/126.8/147.6/154.6 (C_{ar}), 173.3 (*C*OOH). For mass spectroscopy and elemental analyses see table 7.

6.2.3.3. *3,4,5-Tris(perfluoroalkylalkoxy)benzoic acids* ***K3S***

Example of spectral data, for 3,4,5-tris(perfluorohexyl-octyloxy)benzoic acid **K3S[6,8]**: IR (KBr): ν/cm^{-1}=3400–2400, 2941, 2858, 1696, 1590, 1506, 1471, 1436, 1332, 1237, 1211, 1192, 1145, 1049, 790, 699. ^{1}H NMR: δ (ppm)=1.3–1.7 (m, 30H, (CH_2)$_5$–C$_2$H$_4$–O), 1.7–1.9 (m, 6H, CH_2–CH$_2$–O), 2.05 (tt, [18.7 Hz, 8.4 Hz], 6H, CF$_2$–CH_2), 4.06 (t, [6.4 Hz], 4H, 2x CH_2–O), 4.17 (t, [6.7 Hz], 2H, 1x CH_2–O), 7.33 (s, 2 H_{ar}). ^{13}C NMR: δ (ppm)=20.5 (*C*H$_2$–CH$_2$–CF$_2$), 26.3/29.4–29.7 ((*C*H$_2$)$_5$–CH$_2$–O), 31.2 (t, [22.3 Hz], CF$_2$–*C*H$_2$), 69.4/73.8 (*C*H$_2$–O), 108.9/124.1/143.5/153.2 (C_{ar}), 172.1 (*C*OOH). For mass spectroscopy and elemental analyses see table 7.

6.2.4. Perfluoroalkylalkoxybenzoic succinimidyl (NHS) esters. One equiv. (about 3 mmol) of acid **K1S**, **K2S** or **K3S** was dissolved/suspended in 50 ml dry THF, together with one equiv. of DMAP, 1.2 equiv. of DCC and 1.2 equiv. of *N*-hydroxysuccinimid. The reaction mixture was stirred for about 4 days and every 24 h another 0.2 equiv. of NHS and DCC were added until the acid was no longer detectable on TLC. Usually, the reaction was stopped after about one week. The mixture was then poured into 100 ml methanol and stored at 2°C overnight. The white precipitate was filtered off and recrystallized from ethyl acetate; yield approximately 85%. R_f (cyclohexane/ethyl acetate): **K1NS[8,11]**: R_f (1/1)=0.71; **K1NS[10,5]**: R_f (3/1)=0.39; **K2NS[6,11]**: R_f (3/1)=0.49; **K2NS[8,11]**: R_f (1/1)=0.65; **K3NS[6,11]**: R_f (1/1)=0.84; **K3NS[8,11]**: R_f (1/1)=0.85; **K3NS[10,11]**: not detectable on TLC.

6.2.4.1. *N-uccinimidyl 4-(perfluoroalkylalkoxy) benzoates* ***K1NS***

Example of spectral data, for *N*-succinimidyl 4-(per-fluorooctylundecyloxy)benzoate **K1NS[8,11]**: IR (KBr): ν/cm^{-1}=2925, 2854, 1758, 1753, 1605, 1511, 1471, 1371, 1329, 1257, 1216, 1149, 1070, 984, 847, 755, 656. ^{1}H NMR: δ (ppm)=1.25–1.75 (m, 16 H, (CH_2)$_8$–C$_2$H$_4$–O), 1.82 (pseudo-qi, [7.2 Hz], 2H, CH_2–CH$_2$–O), 2.05 (tt, [7.8 Hz, 18.5 Hz], 2H, CF$_2$–CH_2), 2.91 (s, 4H, CH_2 (succinimidyl)), 4.04 (t, [6.6 Hz], 2H, CH_2–O), 6.95 (d, [8.5 Hz], 2 H_{ar}*ortho* to C–O–CH$_2$), 8.08 (d, [8.5 Hz], 2 H_{ar}*ortho* to C–COO). For mass spectroscopy and elemental analyses see table 7.

6.2.4.2. *N-uccinimidyl 3,4-bis(perfluoroalkylalkoxy) benzoates* ***K2NS***

Example of spectral data, for *N*-succinimidyl 3,4-bis(perfluorooctylundecyloxy)benzoate **K2NS[8,11]**: IR (KBr): ν/cm^{-1}=2924, 2854, 1767, 1742, 1735, 1274, 1246, 1203, 1151, 1135, 1076, 751, 705, 658. ^{1}H NMR: δ (ppm)=1.2–1.7 (m, 32H, (CH_2)$_8$–C$_2$H$_4$–O), 1.86/1.89 (2x pseudo-qi, [6.2 Hz], 4H, CH_2–CH$_2$–O), 2.05 (tt, [19 Hz, 7.2 Hz], 4H, CH_2–CF$_2$), 2.90 (s, 4H, CH_2 (succinimidyl)), 4.03/4.08 (2x t, [6.5 Hz], 4H, 2x CH_2–O), 6.91 (d, [6.5 Hz], 1 H_{ar}), 7.56 (d, [2.0 Hz], 1 H_{ar}), 7.77 (dd, [6.5 Hz, 2.0 Hz], 1 H_{ar}). ^{13}C NMR: δ (ppm)=20.2 (*C*H$_2$–CH$_2$–CF$_2$), 25.6 (*C*H$_2$ (*N*-succinimidyl)), 26.2/29.2/29.4/29.5/29.6/ 29.6/29.8 ((CH$_2$)$_8$–CH$_2$–O), 30.8 (t, [22.5 Hz], *C*H$_2$–CF$_2$), 69.2, 69.5 (*C*H$_2$–O), 112.0/114.6/117.0/125.2/149.1/155.1 (C_{ar}), 161.8 (O–*C*O), 169.5 (*C*O–N–*C*O). For mass spectroscopy and elemental analyses see table 7.

6.2.4.3. *N-uccinimidyl 3,4,5-tris(perfluoroalkylalkoxy) benzoates* ***K3NS***

Example of spectral data (succinimidyl 3,4,5-tris(per-fluorooctylundecyloxy)benzoate **K3NS[8,11]**): IR (KBr): ν/cm^{-1}=2922, 2853, 1766, 1740, 1627, 1587, 1499, 1470, 1433, 1372, 1336, 1238, 1205, 1151, 1135, 1118, 1076, 1052, 705, 657. ^{1}H NMR: δ (ppm)=1.2–1.7 (m, 48H, (CH_2)$_8$–C$_2$H$_4$–O), 1.82 (3x pseudo-qi, [6.9 Hz], 6H, CH_2–CH$_2$–O), 2.08 (tt, [20.6 Hz, 8.5 Hz], 6H, CH_2–CF$_2$), 2.92 (s, 4H, CH_2 (succinimidyl)), 4.01/4.05 (2x t, [5.9 Hz], 4H+2H, CH_2–O), 7.33 (s, 2 H_{ar}). For mass spectroscopy and elemental analyses see table 7.

Acknowledgements

We gratefully acknowledge the financial support of the Deutsche Forschungsgemeinschaft (La 662/7,1;7,2) and of TEMPUS (JEP-12387-97).

References

[1] F. Guittard, S. Geribaldi. *J. fluorine Chem.*, **107**, 363 (2001); F. Guittard, E. Taffin de Givenchy, S. Geribaldi and A. Cambon. *J. fluorine Chem.*, **100**, 85 (1999).

[2] H.T. Nguyen, G. Sigaud, M.F. Achard, F. Hardouin, R.J. Twieg, K. Betterton. *Liq. Cryst.*, **10**, 389 (1991).

[3] J.F. Rabolt, T.P. Russell, R.J. Twieg. *Macromolecules*, **17**, 2786 (1984); T.P. Russell, J.F. Rabolt, R.J. Twieg, R.L. Siemens, B.L. Farmer. *Macromolecules*, **19**, 1135 (1986); P. Marczuk, P. Lang. *Macromolecules*, **31**, 9013 (1998); P. Kirsch, M. Bremer. *Angew. Chem.*, **112**, 4384 (2000); *Angew. Chem. int. Ed.*, **39**, 4216.

[4] For micellar systems see, for example: P. Metrangolo, T. Pilati, G. Resnati, A. Stevenazzi. *Curr. Opin. colloid interface Sci.*, **8**, 215 (2003); P. Lo Nostro. *Curr. Opin. colloid interface Sci.*, **8**, 223 (2003).

[5] H. Okamoto, N. Yamada, S. Takenaka. *J. fluorine Chem.*, **91**, 125 (1998); H. Okamoto, H. Murai, S. Takenaka. *Bull. chem. Soc. Jpn.*, **70**, 3163 (1997); F.G. Tournilhac, L. Bosio, J. Simon, L.M. Blinov, S.V. Yablonsky. *Liq. Cryst.*, **14**, 405 (1993).

[6] V. Percec, D. Schlueter, G. Ungar. *Macromolecules*, **30**, 645 (1997); A. Pegenau, Xiao Hong. Cheng, C. Tschierske, P. Göring, S. Diele. *New J. Chem.*, **23**, 465 (1999); M.-A. Guillevic, C.W. Bruce. *Liq. Cryst.*, **27**, 153 (2000); X.H. Cheng, S. Diele, C. Tschiesrske. *Angew. Chem.*, **112**, 605 (2000); M. Hein, R. Miethchen, D. Schwaebisch, C. Schick. *Liq. Cryst.*, **27**, 163 (2000).

[7] V. Percec, D. Schlueter, Y.K. Kwon, J. Blackwell, M. Möller, P.J. Slangen. *Macromolecules*, **28**, 8807 (1995).

[8] G. Johansson, V. Percec, G. Ungar, J.P. Zhou. *Macromolecules*, **29**, 646 (1996).

[9] V. Percec, G. Johansson, G. Ungar, J. Zhou. *J. Am. chem. Soc.*, **118**, 9855 (1996).

[10] X. Cheng, M.K. Das, S. Diele, C. Tschierske. *Langmuir*, **18**, 6521 (2002).

[11] E. Nishikawa, J. Yamamoto, H. Yokoyama. *Chem. Lett.*, 454 (2001).

[12] C. Tschierske. *J. mater. Chem.*, **11**, 2647 (2001); M. Kölbel, T. Beyersdorff, X.H. Cheng, C. Tschierske. *J. Am. chem. Soc.*, **123**, 6809 (2001); M. Prehm, S. Diele, M.K. Das, C. Tschierske. *J. Am. chem. Soc.*, **125**, 614 (2003); M. Prehm, X.H. Cheng, S. Diele, M.K. Das, C. Tschierske. *J. Am. chem. Soc.*, **124**, 12072 (2002); X.H. Cheng, M.K. Das, S. Diele, C. Tschierske. *Angew. Chem. int Ed.*, **41**, 4031 (2002).

[13] G. Lattermann. *Mol. Cryst. liq. Cryst*, **182B**, 299 (1990); G. Lattermann, S. Schmidt, Gallot. *Chem. Commun.*, **1992**, 1091; A. Facher, U. Stebani, G. Lattermann, S. Diele, M. Neundorf. *Liq. Cryst.*, **25**, 441 (1998).

[14] U. Stebani, G. Lattermann, M. Wittenberg, R. Festag, J.H. Wendorff. *Adv. Mater.*, **6**, 572 and correction: (1994), *Adv. Mater.*, **6**, 790 (1994); U. Stebani, G. Lattermann, R. Festag, M. Wittenberg, J.H. Wendorff. *J. mater. Chem.*, **5**, 2247 (1995); U. Stebani, G. Lattermann. *Adv. Mater.*, **7**, 578 (1995); U. Stebani, G. Lattermann, M. Wittenberg, J.H. Wendorff. *J. mater. Chem.*, **7**, 607 (1997).

[15] J.H. Cameron, A. Facher, G. Lattermann, S. Diele. *Adv. Mater.*, **9**, 398 (1997).

[16] A. Facher. PhD thesis, Universität Bayreuth, Germany (2000).

[17] J.O. Metzger, U. Linker. *Liebigs Ann. Chem.*, 209 (1992).

[18] C.H. Erdelen. PhD thesis, University of Mainz, Germany (1993).

[19] N.O. Brace. *J. fluorine Chem.*, **20**, 313 (1982).

[20] W.P. Neumann. *Synthesis*, 665 (1987).

[21] B. Neises, W. Steglich. *Angew. Chem.*, **90**, 556 (1978).

[22] A. Eisenmann, E. Valaityte, G. Lattermann, *Liq. Cryst.* (submitted).

[23] A. Eisenmann, G. Lattermann, *Liq. Cryst.* (submitted).

[24] M. Duan, H. Okamoto, V.F. Petrov, S. Takenaka. *Bull. chem. Soc. Jpn.*, **71**, 2735 (1998).

[25] G. Johansson, V. Percec, G. Ungar, K. Smith. *Chem. Mater.*, **9**, 164 (1997).

[26] Y.H. Chiang, A.E. Ames, R.A. Gaudiana, T.G. Adams. *Mol. Cryst. liq. Cryst.*, **208**, 85 (1991); R. Twieg, K. Betterton, R. DiPietro, D. Gravert, C. Nguyen, H.T. Nguyen, A. Babeau, C. Destrade, G. Sigaud. *Mol. Cryst. liq. Cryst.*, **217**, 201 (1992).

[27] A. Pegenau, X.H. Cheng, C. Tschierske, P. Göring, S. Diele. *New J. Chem.*, **23**, 465 (1999); U. Dahn, C. Erdelen, H. Ringsdorf, R. Festag, J.H. Wendorff, P.A. Heiney, N.C. Maliszewsky. *Liq. Cryst.*, **19**, 759 (1995).

[28] V. Percec, C.-H. Ahn, W.-D. Cho, A.M. Jamieson, J. Kim, T. Leman, M. Schmidt, M. Gerle, M. Möller, S.A. Prokhorova, S.S. Sheiko, S.Z.D. Cheng, A. Zhang, G. Ungar, D.J.P. Yeardley. *J. Am. chem. Soc.*, **120**, 8619 (1998); M.E. Neubert, S.J. Laskos Jr, L.J. Maurer, L.T. Carlino, J.P. Ferrato. *Mol. Cryst. liq. Cryst.*, **44**, 197 (1978); R.P. Tuffin, K.J. Toyne, J.W. Goodby. *J. Mater. Chem.*, **6**, 1271 (1996).

[29] C. Lautner. Diploma thesis, Universität Bayreuth, Germany (1998).

[30] H.T. Nguyen, J.C. Rouillon, A. Babeau, J.P. Marcerou, G. Sigaud, M. Cotrait, H. Allouchi. *Liq. Cryst.*, **26**, 1007 (1999).

[31] D. Lose, S. Diele, G. Pelzl, E. Dietzmann, W. Weissflog. *Liq. Cryst.*, **24**, 707 (1998); G. Pelzl, S. Diele, D. Lose, B.I. Ostrovski, W. Weissflog. *Cryst. Res. Technol.*, **32**, 99 (1997).

[32] G.W. Gray, J.W.G. Goodby. *Smectic Liquid Crystals* Leonard Hill, Glasgow, p. 7 (1984).

[33] A.I. Kitaigorodsky. *Molecular Crystals and Molecules* Academic Press, New York (1973).

[34] C.S. Marvel, W.E. Garrison, Jr. *J. Am. chem. Soc.*, **81**, 4737 (1959).